



Cite this: *Nanoscale*, 2015, 7, 16798

Broadband near-field enhancement in the macro-periodic and micro-random structure with a hybridized excitation of propagating Bloch-plasmonic and localized surface-plasmonic modes†

Haifei Lu,^{‡a} Xingang Ren,^{‡a} Wei E. I. Sha,^a Ho-Pui Ho^b and Wallace C. H. Choy^{*a}

We demonstrate that the silver nanoplate-based macroscopically periodic (macro-periodic) and microscopically random (micro-random) structure has a broadband near-field enhancement as compared to conventional silver gratings. The specific field enhancement in a wide spectral range (from UV to near-infrared) originates from the abundance of localized surface-plasmonic (LSP) modes in the microscopically random distributed silver nanoplates and propagating Bloch-plasmonic (PBP) modes from the macroscopically periodic pattern. The characterization of polarization dependent spectral absorption, surface-enhanced Raman spectroscopy (SERS), as well as theoretical simulation was conducted to comprehensively understand the features of the broadband spectrum and highly concentrated near-field. The reported macro-periodic and micro-random structure may offer a new route for the design of plasmonic systems for photonic and optoelectronic applications.

Received 22nd May 2015,
Accepted 7th September 2015

DOI: 10.1039/c5nr03391h

www.rsc.org/nanoscale

Introduction

Metal grating structures on the nanoscale have received a great amount of attention and have been applied to various fields because of their extraordinary optical properties from propagating Bloch-plasmonic (PBP) modes. Because of PBP resonance, very strong electric fields are concentrated around the metal nanostructure. In terms of practical applications, the metal nanostructures can be used to increase the effective optical path length and absorption efficiency in the absorber layer of photovoltaic devices.^{1–6} Meanwhile, the strong electric fields around metal nanostructures will also affect the optical properties of nearby materials, which have merits in different applications, such as surface enhanced Raman spectroscopy (SERS) and surface enhanced fluorescence emission, for bio-sensing and lighting applications.^{7–11} However, typically regular periodic metal gratings can only provide limited PBP peaks with narrow bandwidths.^{12,13}

Metal nanostructures with a broadband optical field enhancement, on the other hand, would be of more interest to a wide variety of applications.^{14,15} Recently, the aperiodic or quasi-random nanostructures, which lie between the types of periodic and disordered structures, have been receiving increasingly more attention with the aim to explore their unique optical properties in controlling light propagation and localization. The existence of long-range order in such nanostructures could enrich their optical resonance modes.^{16–20} Surface enhanced Raman scattering, and lasing and sensing applications have been explored to achieve higher efficiency through modulating the light-matter interaction with properties of long range order.^{17,20–30} Furthermore, solar cells with periodic random structures, *i.e.* aperiodic or quasi-crystal nanostructures, have been shown to have more significantly improved performance because of their enriched spectral frequencies.^{31–35} The macroscopically periodic (macro-periodic) and microscopically random (micro-random) silver nanostructures, which also lie between periodic and random structures despite simultaneously breaking translational symmetry and long-range order in the spatial domain, have been theoretically and experimentally investigated in terms of far-field response and diffraction.³⁶

In this study, we show the primary merits of broadband and strong field-enhancement from such silver nanoplate based macro-periodic and micro-random structures through

^aDepartment of Electrical and Electronic Engineering, The University of Hong Kong, Pokfulam Road, Hong Kong SAR, P. R. China. E-mail: chchoy@eee.hku.hk

^bDepartment of Electronic Engineering, The Chinese University of Hong Kong, Shatin, N.T., Hong Kong SAR, P. R. China

†Electronic supplementary information (ESI) available. See DOI: 10.1039/c5nr03391h

‡These authors contributed equally to this work.

experimental and theoretical investigations. Through experimental measurements of SERS under the excitation at difference laser wavelengths, we conducted a comparison between the one-dimensional (1D) macro-periodic and micro-random structure and conventional silver grating. Meanwhile, theoretical near-field distribution of the plasmonic system was studied using the finite-difference frequency-domain (FDFD) method. Indeed experimental as well as theoretical results demonstrated that a strong near-field enhancement over a wide spectral range is present in the reported nanostructure as compared to the conventional silver grating case. The broadband enhancement is due to the excited localized surface-plasmonic (LSP) modes from randomly distributed nanoplates. Moreover, PBP modes from the periodic pattern, hybridized with the LSP modes, enhance the optical field further as indicated by the polarization dependent Raman scattering results. The results reported herein suggest that the macro-periodic and micro-random structure may lead to many application opportunities in photonics and optoelectronics.

Results and discussion

The silver macro-periodic and micro-random nanostructure was grown on a glass substrate in a large area through a seed-initiated photochemical process. Because of the presence of twinned defects in the silver nano-seeds and the use of a low photon energy light source (632.8 nm), silver atoms will deposit on the defect regions due to the high potential energy, which induces the growth of nano-seeds along the twinned planes and their transformation into silver nanoplates with {111} stacking fault planes inside. In addition, the periodicity of the structure can be feasibly altered by adjusting the interfering laser beams' angle of incidence.³⁶ The scanning electron microscopy (SEM) image of one typical sample is shown in Fig. 1(a). The randomly distributed silver nanoplates can be readily distinguished and are periodically arranged on the glass substrate. Because of their size variation and random distribution, a large number of LSP modes can be excited in the silver nanoplates. Hence they result in a broadband optical response from UV to near-infrared shown in Fig. 1(b) and (c), where we show the absorption spectra (1-T-R) obtained with the periodic strips perpendicular (TM) and parallel (TE) to the polarization of the incident light. In addition, a red-shifted resonance peak with increasing incident angle can be clearly observed in Fig. 1(b). This is caused by one of the PBP modes at the silver/air interface, which can be evidenced by the simulation result of perfect silver grating in Fig. S1.†

On the other hand, no obvious peak shift has been observed in the absorption spectra for TE illumination as shown in Fig. 1(c). The optical properties of the sample under TE illumination resemble that of an absolutely random structure. Despite the fact that the structure is comprised of anisotropic nanoplates, the total optical response from LSP modes of silver nanoplates would show less dependency on the polarization of the characterization light, due to their random

distribution and the large area of light beam. Thus, as shown in Fig. 1(d) through subtracting the absorption spectra under TE illumination from the one under TM, their difference, in some degree, can be considered as the absorption induced by the PBP modes caused by the periodicity of the pattern. The PBP excited at the interface of air/silver can be more clearly distinguished as in Fig. 1(d). As indicated by the red and blue arrows, under the oblique incidence, the features of red- and blue-shifts for the two split PBP peaks have also been observed as the incident angle increases, respectively. The shift of PBP peaks in the macro-periodic and micro-random structure is coincident with the trend of PBP modes in perfect grating as illustrated in Fig. S1.† Therefore, the periodic arrangement of the randomly distributed nanoplates has been demonstrated to preserve the propagating Bloch-plasmonic (PBP) modes, which introduces more optical resonance modes than purely random structures, and will broaden and strengthen the optical enhancement of the nanostructure.

Then, the broadband near-field enhancement feature has been investigated through comparing SERS signals from the macro-periodic and micro-random structures with that of conventional silver grating, whose extinction spectra characterized under TM illumination of normal incident light are shown in Fig. 2(a). In the SERS measurement, three excitation wavelengths of 488 nm, 633 nm and 785 nm, and 4-mercaptobenzoic acid (4-MBA) as Raman tags were studied. In order to assess the average field enhancement from the patterns, low magnification objectives ($\times 20$) were used for Raman characterization so that the laser spot covered more than five periodic strips. As shown in Fig. 2(c), the Raman peak at 1586 cm^{-1} (corresponding to 704 nm) under the excitation of 633 nm laser light is quite close to the PBP peak of the conventional silver grating. After calculating the area integral of the Raman peak at 1586 cm^{-1} in Fig. 2(c), the signal intensity in the case of nanoplate-based periodic structure was 1.5 times higher than that of the conventional silver grating. In addition, Raman spectra under the excitation of 488 nm and 785 nm shown in Fig. 2(b) and (d) indicate that the macro-periodic and micro-random structures exhibit a stronger enhancement 3.5 and 9 times than that of conventional silver grating with respect to the Raman peaks at 1586 cm^{-1} and 1076 cm^{-1} respectively. Consequently, our experimental results have revealed a superior SERS signal intensity from the nanoplate-based periodic pattern over a wide spectral range, which can be mainly attributed to the higher near-field enhancement offered by the macro-periodic and micro-random structure compared to the conventional silver grating.

To theoretically understand the optical field enhancement effect of the macro-periodic and micro-random structure, the random nanopattern was studied by solving the Maxwell equations of the system numerically using a combination of supercell approximation³⁷ and Monte Carlo analysis³⁸ implemented with the finite-difference frequency domain (FDFD) algorithm.^{39,40} To simplify the simulation, we adopted a 2D model (680 nm in periodicity, 300 nm in strip width, 50 nm in strip height) by merely considering the cross-

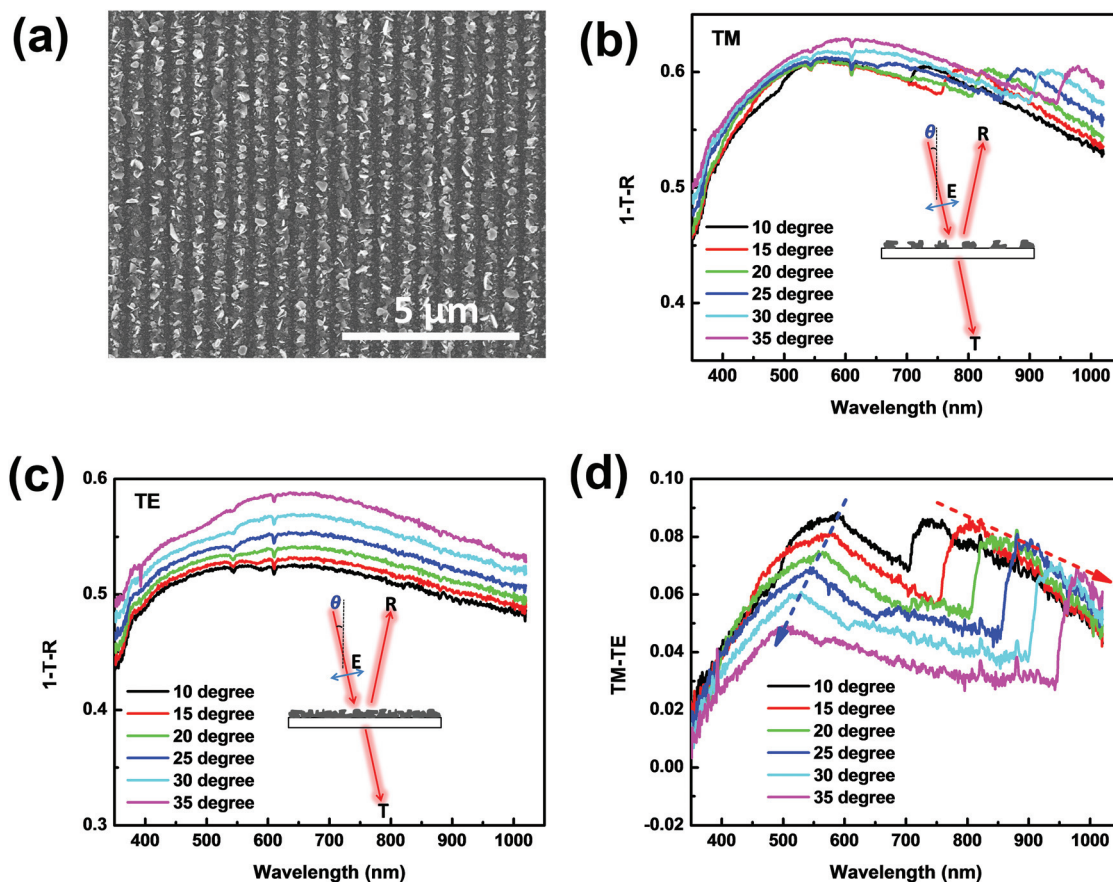


Fig. 1 (a) SEM image and absorption spectra of one typical macro-periodic and micro-random structure (588 nm in periodicity) characterized by p-polarized light with polarization (b) perpendicular (TM) and (c) parallel (TE) to the metal strips. (d) The difference of absorption efficiencies between TM and TE illuminations at different incident angles.

sectional near field distribution and generating multiple random elements in each unit cell (one grating period) to form a supercell (including five unit cells) as shown in Fig. 3(b). The filling factors of silver and air are crucial to the optical response of such macro periodic and micro-random structures.³⁶ With the same fixed filling factors of silver and air as previously reported values (*i.e.* 0.4 and 0.6 respectively),³⁶ the great amount of supercells have been generated by the Monte Carlo method to model the random feature of the macro-periodic and micro-random structure. Here, we choose 785 nm as the excitation wavelength for comparison. Theoretically, the SERS enhancement factor (EF) of metal nanostructure is majorly attributed to the electric field enhancement of two parts: (1) the local field enhancement corresponding to the electric field at the excitation wavelength ($\lambda_{\text{excite}} = 785$ nm, excitation laser wavelength); (2) the radiation field enhancement estimated from the electric field at a Raman emission wavelength of $\lambda_{\text{emit}} = 860$ nm (corresponding to the Raman shift at 1076 cm^{-1}) as shown in Fig. 3. The EF is proportional to the square of the local electric field multiplied by the square of the radiation electric field.⁴¹ Here, a ratio (R) is defined for

comparing the average EF of the nanostructured pattern with the conventional grating as follows:

$$R = \frac{\sum_{i=1}^n \left[\frac{E_{\text{ran}}(\lambda_{\text{excite}}) \cdot E_{\text{ran}}(\lambda_{\text{emit}})}{E_{\text{inc}}(\lambda_{\text{excite}}) \cdot E_{\text{inc}}(\lambda_{\text{emit}})} \right]_i^2}{\sum_{i=1}^n \left[\frac{E_{\text{con}}(\lambda_{\text{excite}}) \cdot E_{\text{con}}(\lambda_{\text{emit}})}{E_{\text{inc}}(\lambda_{\text{excite}}) \cdot E_{\text{inc}}(\lambda_{\text{emit}})} \right]_i^2} = \frac{\sum_{i=1}^n [E_{\text{ran}}(\lambda_{\text{excite}}) \cdot E_{\text{ran}}(\lambda_{\text{emit}})]_i^2}{\sum_{i=1}^n [E_{\text{con}}(\lambda_{\text{excite}}) \cdot E_{\text{con}}(\lambda_{\text{emit}})]_i^2},$$

where $E_{\text{ran}}(\lambda_{\text{excite}})$ and $E_{\text{ran}}(\lambda_{\text{emit}})$ are the electric fields at the excitation and emission wavelengths for the macro-periodic and micro-random patterns, respectively, and $E_{\text{con}}(\lambda_{\text{excite}})$ and $E_{\text{con}}(\lambda_{\text{emit}})$ correspond to those of the conventional silver grating. The ratio (R) is obtained through dividing the summation of EF at all the positions above the silver micro-random structure by that of the conventional grating. Finally, the average EF ratio (R) converges to 11.4 after simulating 120 random structures using the Monte Carlo method. In addition, using a similar simulation approach, the SERS average EF ratios under 488 nm and 633 nm excitation are calculated to be 5.5 and 1.6 respectively as shown in Table 1. The relative low average EF ratio under 633 nm excitation can be attributed

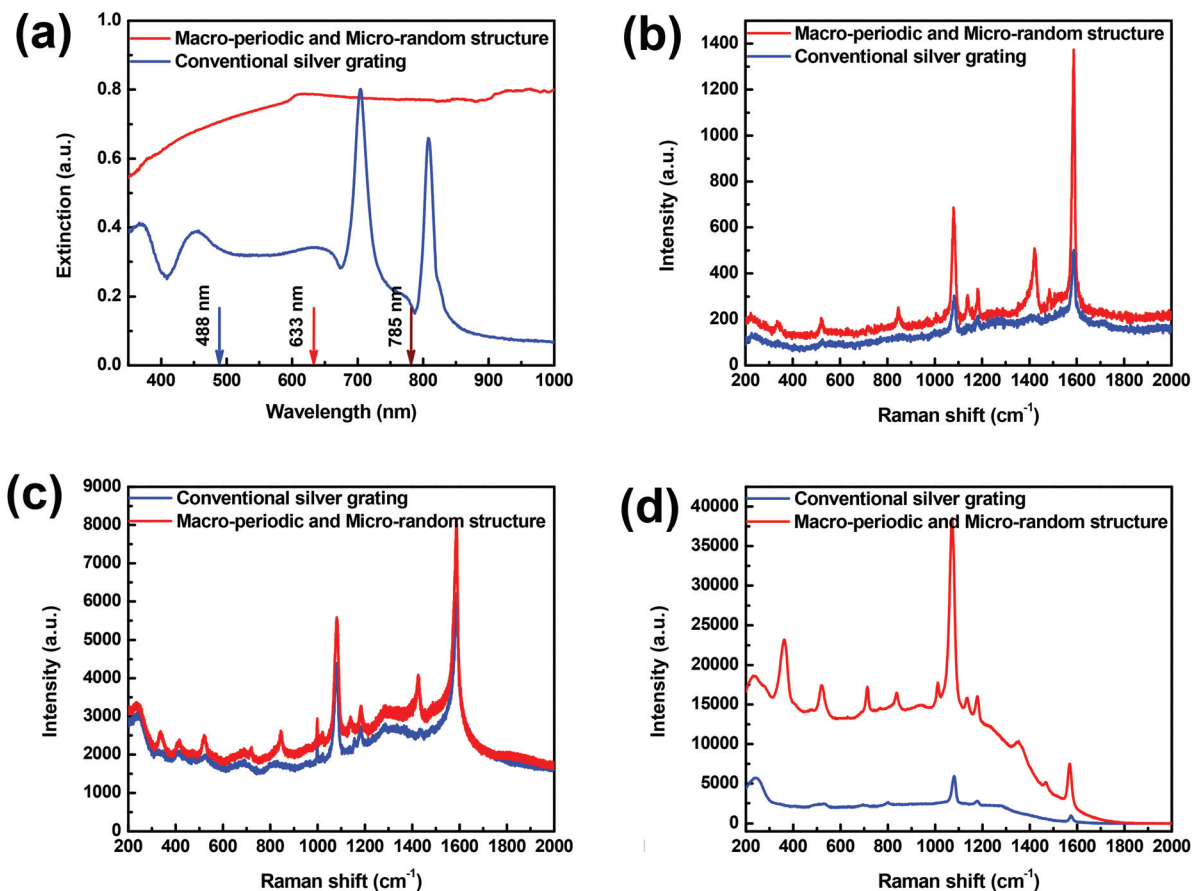


Fig. 2 (a) Extinction spectra of conventional and macro-periodic and micro-random silver nanoplate based structure. (b–d) Their Raman spectra with the excitation of 488 nm, 633 nm and 785 nm lasers respectively.

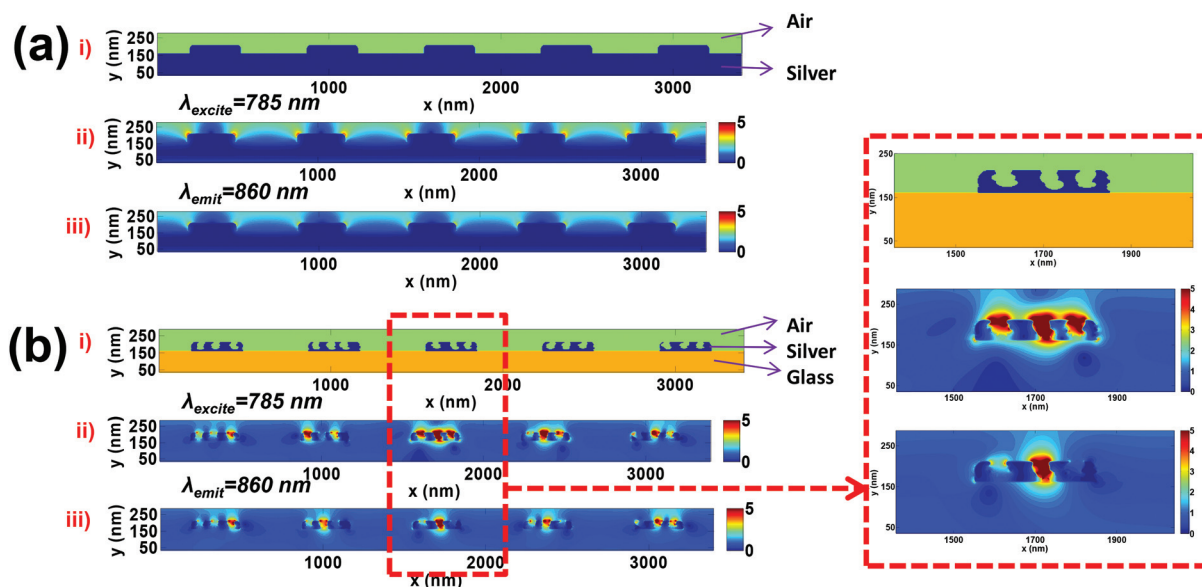


Fig. 3 Structures and the corresponding simulated electric field profiles of (a) conventional grating and (b) supercell of a typical macro-periodic and micro-random structure at 785 nm and 860 nm, with an enlarged cell in (b) for better view. a(i) and b(i) are structural profiles, a(ii) and b(ii) are electric field profiles at an excitation wavelength of 785 nm, and a(iii) and b(iii) are electric field profiles at an emission wavelength of 860 nm.

Table 1 Simulated and experimental average EF ratios of the macro-periodic and micro-random structure to conventional silver grating under 488 nm, 633 nm and 785 nm excitation

Average EF	488 nm	633 nm	785 nm
Simulation ratio	5.5	1.6	11.4
Experiment ratio	3.5	1.5	9

to the high optical field enhancement of conventional silver grating at a wavelength of Raman emission of 1586 cm^{-1} (corresponding to 704 nm), which is quite close to the PBP mode of the conventional silver grating as shown in Fig. 2(a). The experimental SERS enhancement as well as the theoretical ratio of the average EF confirms that the macro-periodic and micro-random structure can offer much higher field enhancement as compared to that of the conventional grating. As evidenced by one typical electric field distribution in Fig. 3(a), the hot-spots only occur at the corners for the conventional grating, whereas more hot-spots are present in the micro-random structures as shown in Fig. 3(b), which will strengthen their field enhancement effect definitely. In the ESI,[†] we also show the electric field distribution of the same typical random nanostructured pattern and conventional grating under the excitation of 488 nm, and 633 nm and their corresponding emission wavelengths.

Because of the broad LSP plasmonic response, the frequency of PBP plasmonic mode would easily overlap with the LSP modes, which allows the hybridized excitation of the modes by the same wavelength of light. To understand the near-field enhancement contributed by the hybridized excitation of plasmonic modes in the macro-periodic and micro-random nanostructure, we measured the polarization dependent Raman spectra from a 1D silver nanoplate-based periodic structure. With the consideration that the PBP mode from the interface of silver/glass can be easily extended to longer wavelength (larger than 900 nm), we choose a sample with the PBP mode from the silver/air interface (790 nm) close to the wavelength of the excitation laser (785 nm). The extinction spectra characterized under TE and TM illumination have been provided as shown in Fig. S3.[†] Through changing the polarization angle that was defined as the angle between the polarized direction of the E-field at 785 nm laser and the lateral direction of periodic strips, a series of Raman spectra have been obtained as shown in Fig. 4(a). As depicted in Fig. 4(b), the Raman signals obtained at different angles all exhibit a relatively high intensity through calculating the area integral of the 1076 cm^{-1} peak. Interestingly, the Raman signals oscillate sinusoidally with increasing polarization angle. The highest signal intensity occurs at the polarization angles of 90 and 270 degrees, which means that the polarization direction of the excitation laser is perpendicular to the periodic strips (namely, TM excitation). The oblique polarization angle will result in the weakened PBP mode, which induces the decrease of the Raman signal intensity. When the

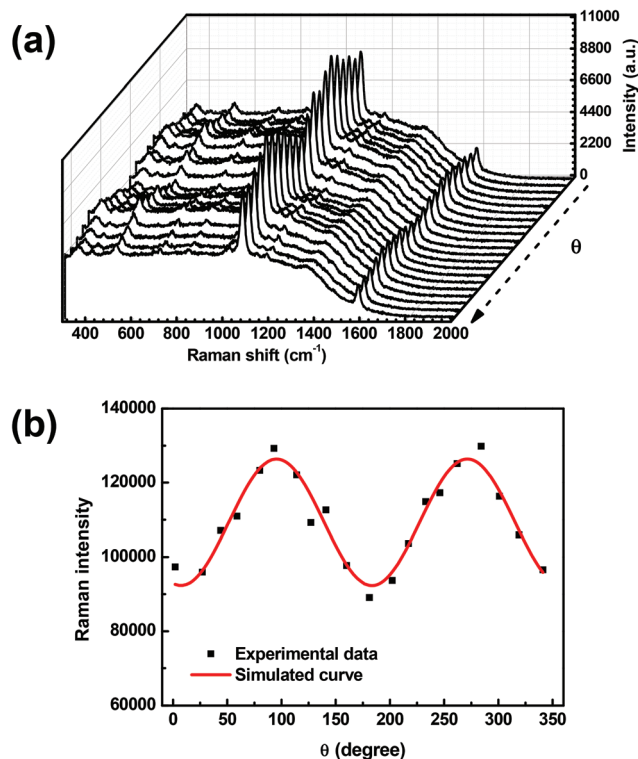


Fig. 4 (a) A series of Raman spectra of 4-MBA on a macro-periodic and micro-random structure at different angles between light polarization and periodic strips. (b) Raman intensity variation with the angle. The red curve is fitted from the experimental data.

polarized direction is parallel to the periodic strips (namely, TE excitation), the Raman intensity reaches the minimum value.

In fact, the Raman spectra obtained with a TE excitation can be considered as a contribution solely from the LSP modes of the random silver nanoplates; and the PBP modes cannot be excited significantly. Therefore, the direct evidence of Raman intensity variation upon changing the polarization angle indicates that the PBP mode readily offers additional near-field enhancement of our nanostructure. Furthermore, we also adopt a simple numerical simulation to reveal the hybridization effect on near field enhancement. As the results indicated in Fig. S4,[†] the periodic arrangement of the micro-random structure can achieve a higher near field intensity as compared to the single strip of a micro-random structure due to the excitation of PBP modes. Finally, it has been demonstrated that the hybridized excitation of LSP and PBP modes in the macro-periodic and micro-random nanostructure would provide the highest near-field enhancement. As the macroscopic period can be easily tuned from 500 nm to several micrometers with appropriate fabrication conditions, PBP modes are able to be engineered for achieving higher field enhancement at specific frequency. One also needs to note that by using such a photochemical approach, a two-dimensional macro-periodic and micro-random structure can also be

easily fabricated to meet more of the requirements in practical applications, such as polarization independent near-field enhancement.

Conclusion

In conclusion, we have experimentally and theoretically investigated the near-field enhancement of the macro-periodic and micro-random silver nanoplate structures. Our experimental results show that the averaged EF of SERS from the macro-periodic and micro-random nanostructure has 3.5, 1.5 and 9 times improvement over that from the conventional grating under laser excitation at the wavelengths of 488 nm, 633 nm and 785 nm, respectively. Remarkably, because of the hybridized excitation of PBP and LSP modes in macro-periodic and micro-random structures, their optical near-fields have been effectively broadened and strengthened as demonstrated by the polarization dependent absorption spectra and SERS features. Consequently, the proposed macro-periodic and micro-random silver nanostructures with a strong near-field enhancement over a wide spectral region would be beneficial to applications in photonic and optoelectronic devices.

Experimental section

The silver nanoplate-based macro-periodic and micro-random structure was fabricated according to a previous report.³⁶ Typically, a glass substrate modified with a layer of small silver nanoparticles was fixed on a glass prism with the metal layer exposed to the reaction solution filled in a PDMS chamber. A mixture of silver nitrate (0.4 mM) and sodium citrate (2.5 mM) aqueous solution was used as the reaction solution. The glass prism and the substrate were placed on a rotation stage, which was used to adjust the incident angle of the expanded 632.8 nm laser beam. After light illumination, the 1D periodic nanostructure with a specific periodicity will gradually form on the glass substrate depending on the incident angle. The conventional silver grating was prepared by thermally evaporating 100 nm silver on a PDMS template with an 1D periodic pattern.

The sample morphology was investigated by using a LEO 1530 FEG scanning electron microscope. The optical extinction and absorption spectra were obtained from a home built goniometer. To characterize the SERS properties of the nanoplate-based macro-periodic and micro-random structures and conventional silver grating, 20 μ L of 4-MBA in ethanol (0.002 mM) were dropped on the two samples respectively, and allowed to dry before Raman spectroscopy measurements. Three lasers (488 nm, 633 nm, and 785 nm) have been used to excite the samples for Raman characterization, and the areas of laser beam are large enough to cover more than 5 periodic strips. In addition, a series of Raman spectra (785 nm excitation) from the same position of the silver nanoplate-based macro-periodic and micro-random structure were acquired by rotating the

sample for different angles between the polarization of excitation laser and the periodic strips. In each measurement, the laser spot on the sample was of the same size.

Acknowledgements

This study was supported by the General Research Fund (grants HKU711813 and HKU711612E), the Collaborative Research Fund (grants: C7045-14E, CUHK1/CRF/12G) and RGC-NSFC grant (N_HKU709/12) from the Research Grants Council of Hong Kong Special Administrative Region, China, and grant CAS14601 from the CAS-Croucher Funding Scheme for the Joint Laboratories.

References

- 1 H. A. Atwater and A. Polman, *Nat. Mater.*, 2010, **9**(3), 205.
- 2 M. A. Green and S. Pillai, *Nat. Photonics*, 2012, **6**(3), 130.
- 3 X. H. Li, W. C. H. Choy, L. J. Huo, F. X. Xie, W. E. I. Sha, B. F. Ding, X. Guo, Y. F. Li, J. H. Hou, J. B. You and Y. Yang, *Adv. Mater.*, 2012, **24**(22), 3046.
- 4 X. H. Li, W. C. H. Choy, X. G. Ren, J. Z. Xin, P. Lin and D. C. W. Leung, *Appl. Phys. Lett.*, 2013, **102**(15), 153304.
- 5 J. B. You, X. H. Li, F. X. Xie, W. E. I. Sha, J. H. W. Kwong, G. Li, W. C. H. Choy and Y. Yang, *Adv. Energy Mater.*, 2012, **2**(10), 1203.
- 6 W. Wang, S. M. Wu, K. Reinhardt, Y. L. Lu and S. C. Chen, *Nano Lett.*, 2010, **10**(6), 2012.
- 7 K. C. Bantz, A. F. Meyer, N. J. Wittenberg, H. Im, O. Kurtulus, S. H. Lee, N. C. Lindquist, S. H. Oh and C. L. Haynes, *Phys. Chem. Chem. Phys.*, 2011, **13**(24), 11551.
- 8 C. Hoppener and L. Novotny, *Q. Rev. Biophys.*, 2012, **45**(2), 209.
- 9 K. Okamoto, I. Niki, A. Shvartser, Y. Narukawa, T. Mukai and A. Scherer, *Nat. Mater.*, 2004, **3**(9), 601.
- 10 M. K. Kwon, J. Y. Kim, B. H. Kim, I. K. Park, C. Y. Cho, C. C. Byeon and S. J. Park, *Adv. Mater.*, 2008, **20**(7), 1253.
- 11 Y. G. Bi, J. Feng, Y. F. Li, X. L. Zhang, Y. F. Liu, Y. Jin and H. B. Sun, *Adv. Mater.*, 2013, **25**(48), 6969.
- 12 V. E. Ferry, J. N. Munday and H. A. Atwater, *Adv. Mater.*, 2010, **22**(43), 4794.
- 13 J. N. Munday and H. A. Atwater, *Nano Lett.*, 2011, **11**(6), 2195.
- 14 K. Aydin, V. E. Ferry, R. M. Briggs and H. A. Atwater, *Nat. Commun.*, 2011, **2**, 517.
- 15 A. S. Hall, M. Faryad, G. D. Barber, L. Liu, S. Erten, T. S. Mayer, A. Lakhtakia and T. E. Mallouk, *ACS Nano*, 2013, **7**(6), 4995.
- 16 M. Segev, Y. Silberberg and D. N. Christodoulides, *Nat. Photonics*, 2013, **7**(3), 197.
- 17 L. Dal Negro and S. V. Boriskina, *Laser Photonics Rev.*, 2012, **6**(2), 178.
- 18 D. S. Wiersma, *Nat. Photonics*, 2013, **7**(3), 188.

- 19 Z. V. Vardeny, A. Nahata and A. Agrawal, *Nat. Photonics*, 2013, **7**(3), 177.
- 20 L. Mahler, A. Tredicucci, F. Beltram, C. Walther, J. Faist, H. E. Beere, D. A. Ritchie and D. S. Wiersma, *Nat. Photonics*, 2010, **4**(3), 165.
- 21 A. Gopinath, S. V. Boriskina, B. M. Reinhard and L. Dal Negro, *Opt. Express*, 2009, **17**(5), 3741.
- 22 B. Yan, A. Thubagere, W. R. Premasiri, L. D. Ziegler, L. Dal Negro and B. M. Reinhard, *ACS Nano*, 2009, **3**(5), 1190.
- 23 L. L. Yang, B. Yan, W. R. Premasiri, L. D. Ziegler, L. Dal Negro and B. M. Reinhard, *Adv. Funct. Mater.*, 2010, **20**(16), 2619.
- 24 A. Gopinath, S. V. Boriskina, N. N. Feng, B. M. Reinhard and L. Dal Negro, *Nano Lett.*, 2008, **8**(8), 2423.
- 25 A. Gopinath, S. V. Boriskina, W. R. Premasiri, L. Ziegler, B. M. Reinhard and L. Dal Negro, *Nano Lett.*, 2009, **9**(11), 3922.
- 26 S. Y. Lee, J. J. Amsden, S. V. Boriskina, A. Gopinath, A. Mitropoulos, D. L. Kaplan, F. G. Omenetto and L. Dal Negro, *Proc. Natl. Acad. Sci. U. S. A.*, 2010, **107**(27), 12086.
- 27 H. Noh, J. K. Yang, S. F. Liew, M. J. Rooks, G. S. Solomon and H. Cao, *Phys. Rev. Lett.*, 2011, **106**(18), 183901.
- 28 M. Notomi, H. Suzuki, T. Tamamura and K. Edagawa, *Phys. Rev. Lett.*, 2004, **92**(12), 123906.
- 29 S. K. Kim, J. H. Lee, S. H. Kim, I. K. Hwang, Y. H. Lee and S. B. Kim, *Appl. Phys. Lett.*, 2005, **86**(3), 031101.
- 30 J. K. Yang, S. V. Boriskina, H. Noh, M. J. Rooks, G. S. Solomon, L. Dal Negro and H. Cao, *Appl. Phys. Lett.*, 2010, **97**(22), 223101.
- 31 R. A. Pala, J. S. Q. Liu, E. S. Barnard, D. Askarov, E. C. Garnett, S. H. Fan and M. L. Brongersma, *Nat. Commun.*, 2013, **4**, 2095.
- 32 E. R. Academic RadiologyMartins, J. T. Li, Y. K. Liu, V. Depauw, Z. X. Chen, J. Y. Zhou and T. F. Krauss, *Nat. Commun.*, 2013, **4**, 2665.
- 33 I. Dolev, M. Volodarsky, G. Porat and A. Arie, *Opt. Lett.*, 2011, **36**(9), 1584.
- 34 V. E. Ferry, M. A. Verschuuren, M. C. van Lare, R. E. I. Schropp, H. A. Atwater and A. Polman, *Nano Lett.*, 2011, **11**(10), 4239.
- 35 K. Vynck, M. Buresi, F. Riboli and D. S. Wiersma, *Nat. Mater.*, 2012, **11**(12), 1017.
- 36 H. Lu, X. Ren, W. E. I. Sha, J. Chen, Z. Kang, H. Zhang, H. P. Ho and W. C. H. Choy, *Sci. Rep.*, 2015, **5**, 7876.
- 37 J. D. Joannopoulos, S. G. Johnson, J. N. Winn and R. D. Meade, *Photonic Crystals Molding the Flow of Light*, Princeton University Press, Woodstock, 2008.
- 38 M. N. O. Sadiku, *Monte Carlo methods for electromagnetics*, CRC Press, Boca Raton, 2009.
- 39 W. E. I. Sha, W. C. H. Choy and W. C. Chew, *Opt. Express*, 2010, **18**(6), 5993.
- 40 X. G. Ren, Z. X. Huang, X. L. Wu, S. L. Lu, H. Wang, L. Wu and S. Li, *Comput. Phys. Commun.*, 2012, **183**(6), 1192.
- 41 E. C. L. Ru and P. G. Etchegoin, *Principles of Surface-Enhanced Raman spectroscopy and related plasmonic effects*, Elsevier, Amsterdam, 2009.